The Contribution of Low-Surface-Brightness Galaxies to Faint Galaxy Number Counts

H.C.Ferguson
Space Telescope Science Institute
S.S. McGaugh
Institute of Astronomy, Cambridge

Low surface-brightness (LSB) galaxies are systematically underrepresented in most low-redshift galaxy surveys. However, deep surveys probe to much deeper isophotal levels, and hence could *in principle* include low-surface-brightness galaxies missed in the local surveys. To explore the consequences of including LSB galaxies, we construct catalogs of simulated *non-evolving* galaxies drawn from a multivariate distribution of galaxy luminosities, central surface brightnesses, bulge/disk ratios and spectral-energy distributions. The model galaxies are convolved with seeing and selected in a manner that closely matches real surveys.

We find it possible to include a large population of LSB galaxies and incorporate a steep faint-end slope of the luminosity function in our simulations without violating the constraints on the local field-galaxy luminosity function or the HI mass function. The most favorable model matches counts, colors and redshift distributions to $B = 23$, but predicts larger effective radii than observed. A realistic non-evolving model is probably somewhere between this extreme model and the standard no-evolution model, which ignores isophotal selection. The results suggest that LSB galaxies could contribute significantly to the counts fainter than $B = 20$, but cannot by themselves reconcile a non-evolving $q_0 = 0.5$ model to the faint-galaxy data. Nevertheless, **inclusion of LSB galaxies could significantly reduce the need for extreme models of evolution such as rapid merging or bursting dwarf galaxies**.

Presented at *Quantifying Galaxy Morphology at High Redshift*, a workshop held at the Space Telescope Science Institute, Baltimore MD, April 27–29 1994

1 Introduction

The counts of faint galaxies in the B and I bands show numbers are well in excess of cosmological models that do not include galaxy evolution, for any value of the deceleration parameter q_0 (Tyson & Jarvis 1979; Tyson 1988; Lilly, Cowie, & Gardner 1991; Metcalfe et al. 1991). Models involving simple passive evolution of galaxies (Tinsley 1980; Bruzual & Kron 1980; Yoshii & Takahara 1988; Guiderdoni & Rocca-Volmerange 1990), predict a high-redshift tail to the redshift distribution at $B > 21$ that is not observed (Broadhurst, Ellis, & Shanks 1988; Colless et al. 1990; Cowie, Songaila, & Hu 1991; Colless et al. 1993). Furthermore, while the B counts show a strong excess over non-evolving models, counts in the K band show no excess (Gardner, Cowie, & Wainscoat 1993). Proposed explanations involve a modification of cosmology through a non-zero cosmological constant, rapid merging of galaxies between redshifts of $z \sim 0.5$ and the present (Guiderdoni & Rocca-Volmerange 1991; Broadhurst, Ellis, & Glazebrook 1992), or rapid luminosity evolution of low-luminosity galaxies over similar timescales (Broadhurst, Ellis, & Shanks 1988; Babul & Rees 1992).

A more conservative suggestion is that plausible modifications to the local luminosity function and distribution of galaxy types can bring no-evolution (NE) models much closer to the data (Driver et al. 1994; Koo, Gronwall, & Bruzual 1993). In this contribution, we propose a specific selection effect that could account for the discrepancy between the local galaxy properties and the deep counts. The crux of our model is the observation that the rest-frame isophotal limits of deep CCD surveys are fainter than the isophotal limits of the photographic surveys used to define the local luminosity function (McGaugh 1994). This is illustrated in Fig. 1, where we show the local and deep survey limits for three galaxies with the same total magnitude but with different scale lengths. Because the intrinsic distribution of surface brightness of disks our goal is to test whether low-surface-brightness (LSB) galaxies can *in principle* contribute significantly to faint-galaxy counts.

2 Models

Figure 2 shows three possibilitiies for the central surface brightness distribution of galaxy disks. The "NE" model corresponds to the standard assumption that surveys are limited by total magnitude. The two other models show plausible distributions of central surface brightness that are consistent with the available data on local field galaxies.

The simplest way to include intrinsic scatter into the galaxy distribution functions is to construct simulated galaxies using Monte-Carlo techniques. For the three models described

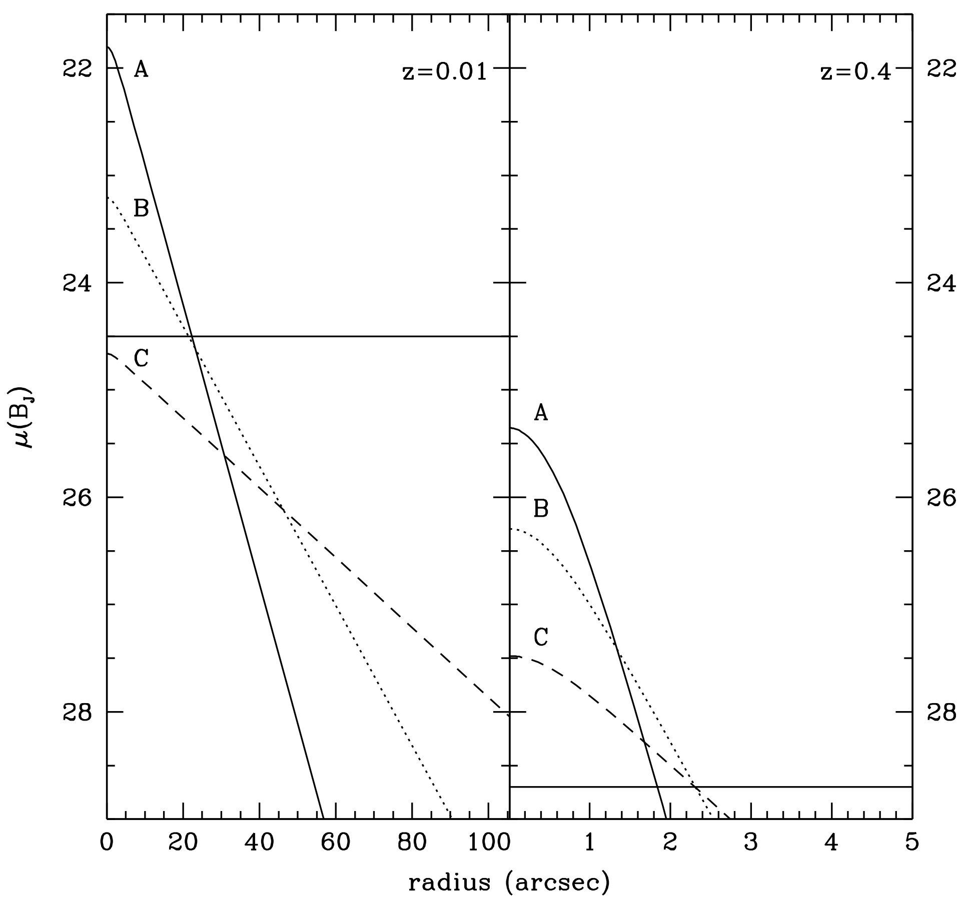

Figure 1:
This figure shows simulated radial surface-brightness profiles for three exponential disk galaxies with ($M_{B_J} = -19$). Galaxy A has the canonical Freeman central surface brightness $\mu_0(B_J) = 21.6$ at $z = 0$. Galaxies B and C have scale lengths a factor of 2 and 4 larger, respectively. The left panel shows the galaxies viewed in 3 arcsec (FWHM) seeing at $z = 0.01$. The horizontal line shows the isophotal threshold of APM survey (Loveday et al. 1992). Galaxy C would be missed entirely by the survey, while galaxy B would have a measured "total" magnitude too faint by 0.7 mag, if the isophotal-to-total correction were based on galaxy A. The right panel shows the same three galaxies shifted to $z = 0.4$ and viewed in 1″seeing. A type II (see text) SED was assumed, giving 1.07 mag of k dimming. The horizontal line in this panel is Tyson's (1988) isophotal threshold $\mu_{B_J} = 28.7$. All three galaxies would be detected above this threshold. Isophotal-to-total magnitude corrections are 0.1, 0.2, and 1.0 mag for galaxies A,B, and C, respectively.

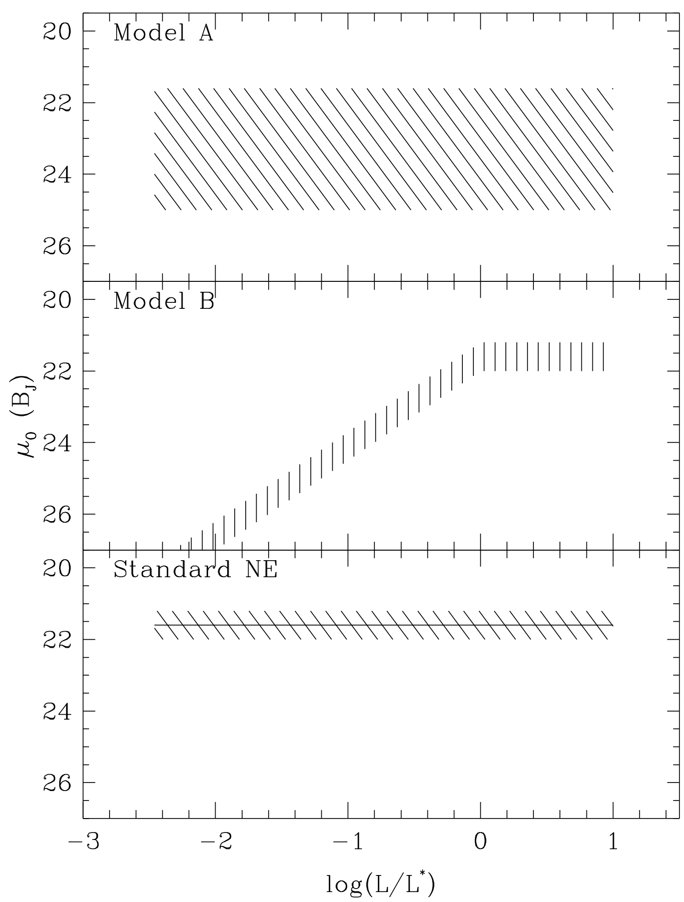

Figure 2: Schematic illustration of the central-surface-brightness distributions assumed for galaxy disks in our models. In model A, we assume that surface-brightness is independent of luminosity. In model B, surface brightness depends on luminosity as described in the text, with 0.4 mag scatter about the mean relation. The Monte-Carlo NE model assumes Freeman disks with 0.4 mag scatter. The analytic NE model assumes no scatter.

below galaxy parameters are chosen at random from the distribution functions describing space density (constant), luminosity, surface brightness, morphological type, and bulge/disk ratio. Catalogs of simulated galaxies are constructed and are observed (i.e. they are selected and their magnitudes are measured) in a way that closely matches real surveys. Model parameters are described below and summarized in Table 2.

- Schechter Luminosity Function

$$\phi(L) = \phi^*(L/L^*)^\alpha e^{-L/L^*} d(L/L^*)$$

- Exponential disks; $r^{1/4}$-law bulges.
- Bulge surface-brightness follows a relation from Sandage & Perelmuter (1990):

$$\mu_{B_e} = 1.20 \log(L/L*) + 21.16 \pm 0.5$$

- Non-evolving spectral-energy distributions (SED's) from Coleman, Wu, & Weedman (1980). Separate SED's for bulge & disk (see Fig. 3).
- Densities adjusted to match Loveday et al. (1992) survey and give type ratios E:S0:Sab:Sbc:Sdm=10:20:25:25:20 for a survey limited at $B = 16$ (Kirshner et al. 1978).
- Galaxy brightness profiles are convolved with seeing before computing isophotal magnitudes or diameters.
- To compute an HI mass function, we use the following formula for types Sa and later (Briggs 1990):

$$M_{HI} = 3.2 \times 10^{10}(L/L_0)^{0.9} M_\odot \quad \text{with } L/L_0 = 10^{-0.4(M_{BJ}+21.1)}$$

- Three different central-surface-brightness distributions for disks, shown schematically in Fig. 2:

NE model: $\mu_B = 21.6 \pm 0.4$ for all disks

Model A: $N(\mu_B)$ constant from $\mu_B = 21.6$ to 25

Model B: $\mu_B = 21.6 \pm 0.4$ for $L \geq L^*$

$mu_B = 21.6 + 2.5 \log(L/L^*) \pm 0.4$ for $L < L^*$

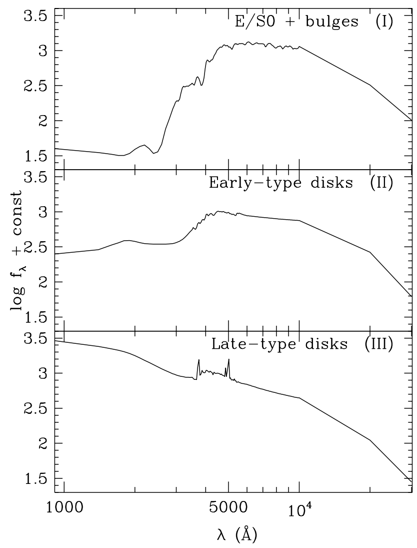

Figure 3: Adopted spectral energy distributions.

- The *type specific* luminosity-function parameters L^* and α were adjusted to produce a total luminosity function that matches that observed by Loveday et al. (1992). The luminosity function for model B is shown in Fig. 4.

The surveys we have chosen to simulate are listed in Table 2. Each is described by the estimated FWHM of the seeing disk, a type of selection (diameter or magnitude), and a type of magnitude (aperture, isophotal, hybrid, or total). We *tune* the model to match roughly the canonical distribution of morphologies and total luminosity function in bright surveys (Table 2 lines 1 & 2). This involves adjusting ϕ^*, L^*, and α separately for the different Hubble types. As an independent test of the properties of local galaxies, we predict the color distributions for a sample of bright galaxies and compare to the observed distribution for a subsample of the RC3 catalog (de Vaucouleurs et al. 1991), finding reasonable agreement. We then compute the faint galaxy counts, redshifts, and colors for the rest of the surveys listed in Table 2.

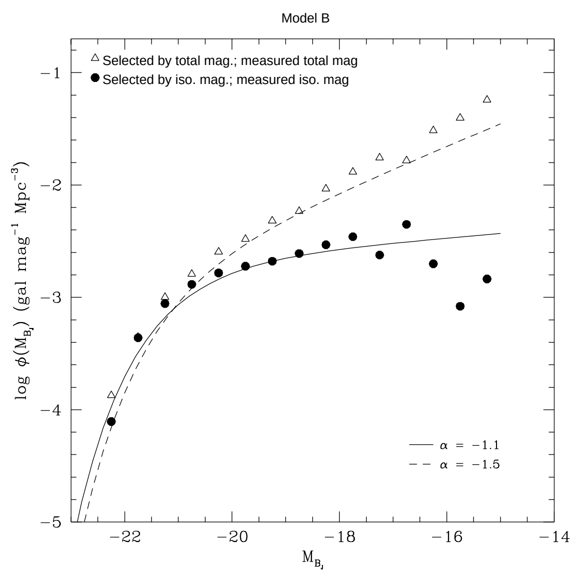

Figure 4: The luminosity function for our model B. The solid line shows our fiducial "observed" total luminosity function, consistent with the APM survey of Loveday et al. (1992). For comparison, the dashed line shows a luminosity function with the same ϕ^*, but with $\alpha = -1.5$. The open symbols show the luminosity function that would be recovered from our simulated galaxy catalogs if galaxies could be selected by total magnitude. The solid symbols show the luminosity function recovered when the APM selection criteria and magnitude estimation scheme are adopted as described in the text. The luminosity functions of the individual morphological types have been tuned to match the fiducial total luminosity function, and comparison here shows the extent to which this tuning has been successful.

Model A

Type	$M_B{}^*$	α	ϕ^* $(10^{-3}\mathrm{Mpc})^{-3}$	bulge to total	Bulge SED	Disk SED
E/S0	-21.1	-1.0	0.35	1.0	I	
S0	-21.1	-1.1	0.71	0.4 ± 0.10	I	I
Sab	-21.1	-0.5	0.97	0.3 ± 0.08	I	II
Sbc	-21.1	-0.5	0.97	0.15 ± 0.04	I	III
Sdm	-20.5	-1.2	0.13	0.0		III

Model B

Type	$M_B{}^*$	α	ϕ^* $(10^{-3}\mathrm{Mpc})^{-3}$	bulge to total	Bulge SED	Disk SED
E/S0	-21.1	-0.5	0.44	1.0	I	
S0	-21.0	-0.5	0.91	0.4 ± 0.10	I	I
Sab	-20.9	-0.5	1.21	0.3 ± 0.08	I	II
Sbc	-20.7	-1.0	1.48	0.15 ± 0.04	I	III
Sdm	-20.6	-1.8	1.44	0.0		III

NE model

Type	$M_B{}^*$	α	ϕ^* $(10^{-3}\mathrm{Mpc})^{-3}$	bulge to total	Bulge SED	Disk SED
E/S0	-21.1	-1.1	0.32	1.0	I	
S0	-21.1	-1.1	0.58	0.4 ± 0.10	I	I
Sab	-21.1	-1.1	0.58	0.3 ± 0.08	I	II
Sbc	-21.1	-1.1	0.58	0.15 ± 0.04	I	III
Sdm	-21.1	-1.1	0.40	0.0		III

Assumed Survey Parameters

Band	Observer	Magnitude	Seeing ($''$)	D_{min} ($''$)	$\mu_{\rm lim}$	
B_J	Loveday	Isophotal	—	3.0	24.5	1
B_J	KOS78	Total	3.0	20	24.5	2
B_J	Tyson	Isophotal	—	1.7	28.7	
B_J	Colless	Isophotal	—	1.0	26.5	3
B_{AB}	Cowie	Isophotal	1.0	1.0	28.6	4
I_{AB}	Lilly N(m)	Hybrid	1.2	2.0	28.0	5
I_{AB}	Lilly N(z)	Aperture	0.7	3.0	28.0	6
K_{AB}	Cowie	Aperture	1.0	3.0	25.4	7

Notes:

1. Correction -0.27 added to isophotal magnitudes.
2. Rough estimates. Used to set type fractions.
3. Correction -0.58 added to isophotal magnitudes.
4. Assumed complete to $D_{28.6} > 2''$. Isophotal magnitudes used.
5. Isophotal magnitudes for galaxies with $D_{28} > 2''$; otherwise, used $2''$aperture.
6. Assumed complete to $D_{28} > 2''$. $3''$aperture magnitudes used.
7. Assumed complete to $D_{25.4} > 1''$. Isophotal magnitudes used.

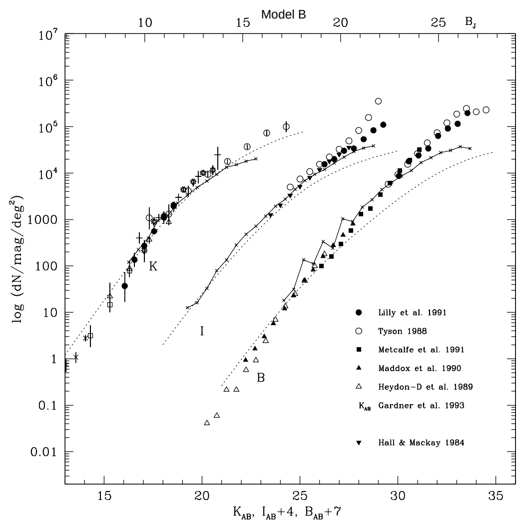

Figure 5: Model number counts in the B_{AB}, I_{AB}, and K_{AB} bands compared to the data from various sources. Solid lines show the expected $N(m)$ for model B. The dashed lines show the standard no-evolution model.

3 Results

Our results are summarized in a paper submitted to the Astrophysical Journal. To save space, we show only the results for Model B here. Galaxy counts are shown in Fig. 5 Redshift distributions are shown in Fig. 6. Faint galaxy colors are shown in Fig. 7. The models have also been used to predict the distribution of axial ratios (Fig. 8) and effective radii and to give an indication of the possible appearance of galaxies in deep WFPC-2 frames.

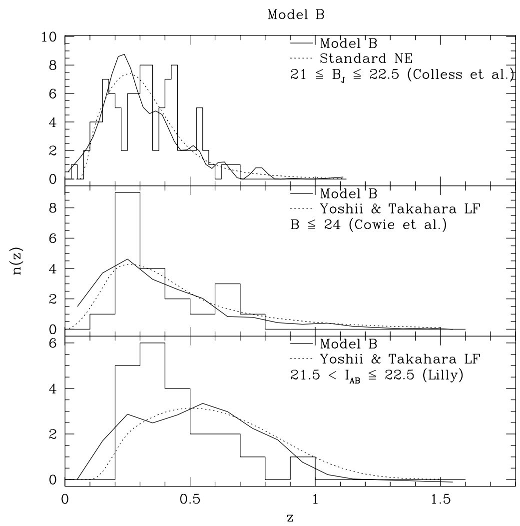

Figure 6: Redshift distributions in the B_J, B_{AB}, and I_{AB} bands. The histograms show the data. The solid curve shows the results of the Model B after simulating the selection criteria of the surveys, and the dotted lines show the result of the standard NE model.

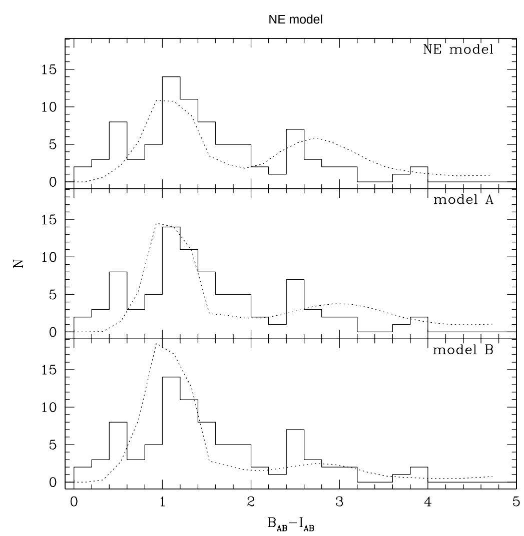

Figure 7: $(B - I)_{AB}$ color distributions for the models limited at $I_{AB} < 25$, compared to the data of Lilly et al. (1991). The models were binned in 0.2 mag intervals, then smoothed with a boxcar filter over 3 bins to simulate photometric errors near the survey limits.

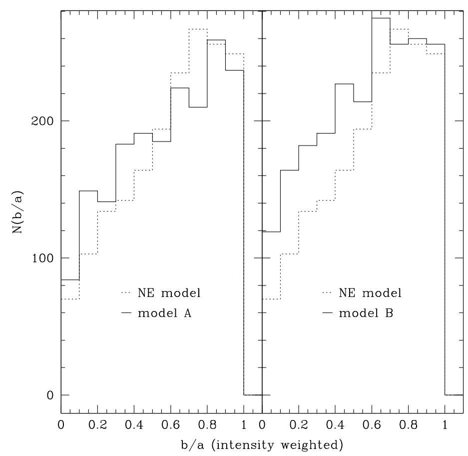

Figure 8: Distribution of intensity-weighted axial ratios (b/a). Galaxies for this sample were selected in the I_{AB} band to have diameters $D_{28} > 1''$ and magnitudes $23 < m_{iso} < 25$. The axial ratio is the weighted mean of the bulge and disk axial ratios, using the flux above the limiting isophote as the weighting factor. The instrumental PSF FWHM is assumed to be $0.1''$. Smearing by this PSF is included in the modeling the selection of galaxies, but not in the computation of their axial ratios.

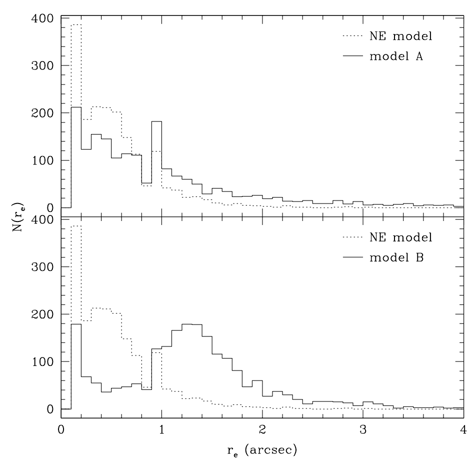

Figure 9: Distribution of half-light radii r_e for the three models. Selection criteria are the same as the previous figure. The computation of r_e includes the effect of smearing by the $0.1''$ PSF.

References

Babul, A. & Rees, M. 1992, MNRAS, 255, 346

Broadhurst, T. J., Ellis, R. S., & Glazebrook, K. 1992, Nature, 355, 55

Broadhurst, T. J., Ellis, R. S., & Shanks, T. S. 1988, MNRAS, 235, 827

Bruzual, A. G. & Kron, R. G. 1980, ApJ, 241, 25

Colless, M., Ellis, R. S., Taylor, K., & Hook, R. N. 1990, MNRAS, 244, 408

Colless, M. M., Ellis, R. S., Broadhurst, T. J., Taylor, K., & Peterson, B. A. 1993, MNRAS, 261, 19

Cowie, L. L., Songaila, A., & Hu, E. M. 1991, Nature, 354, 460

de Vaucouleurs, G., de Vaucouleurs, A., Corwin, H. G. Jr., Buta, R. J., Paturel, G., & Fouqué, P. 1991, The Third Reference Catalog of Bright Galaxies (New York: Springer-Verlag)

Driver, S. P., Phillipps, S., Davies, J. I., Morgan, I., & Disney, M. J. 1994, MNRAS, 266, 155

Gardner, J. P., Cowie, L. L., & Wainscoat, R. J. 1993, ApJ, 415, L9

Guiderdoni, B. & Rocca-Volmerange, B. 1990, A&A, 227, 362

Guiderdoni, B. & Rocca-Volmerange, B. 1991, A&A, 252, 435

Koo, D. C., Gronwall, C., & Bruzual, G. A. 1993, ApJ, 415, L21

Lilly, S. J., Cowie, L. L., & Gardner, J. P. 1991, ApJ, 369, 79

McGaugh, S. S. 1994, Nature, 367, 538

Metcalfe, N., Shanks, T., Fong, R., & Jones, L. R. 1991, MNRAS, 249, 498

Tinsley, B. M. 1980, ApJ, 241, 41

Tyson, J. A. 1988, AJ, 96, 1

Tyson, J. A. & Jarvis, J. F. 1979, ApJ, 230, L153

Yoshii, Y. & Takahara, F. 1988, ApJ, 326, 1